

Spinal Cerebrospinal Fluid Leak Localization with Digital Subtraction Myelography: Tips, Tricks, and Pitfalls



Javier Galvan, MD, MPH^{a,b}, Marcel Maya, MD^{a,b,*}, Ravi S. Prasad, MD^b,
Vikram S. Wadhwa, MD^b, Wouter Schievink, MD^{b,c}

KEYWORDS

- Cerebrospinal fluid leak • Spontaneous intracranial hypotension • Digital subtraction myelography
- MR myelography • CT myelography • Cerebrospinal fluid-venous fistula

KEY POINTS

- Digital subtraction myelography has high sensitivity for identifying leak site.
- A hyperdense paraspinal vein sign may be a false localizing sign of CSF-venous fistulas.
- Paraspinal fluid in the C1-2 region does not correspond to site of CSF leak and is known as the false localizing sign of C1-2.
- CSF leaks in the cervicothoracic region seen on spinal imaging are rarely the site of leak and targeted treatment in this region is not likely to result in lasting symptom relief.
- While rare, skull-based CSF leaks can cause SIH.

 Video content accompanies this article at <http://www.radiologic.theclinics.com>

INTRODUCTION

Cerebrospinal fluid (CSF) leak is a condition in which there is a loss of CSF which leads to spontaneous intracranial hypotension (SIH). SIH can cause a variety of neurologic symptoms, but orthostatic headache due to intracranial hypotension is the most characteristic (**Table 1**).^{1,2} On brain magnetic resonance imaging (MRI), there are characteristic imaging findings associated with intracranial hypotension. These findings encompass subdural fluid collections, pachymeningeal enhancement, engorged venous structures, a hyperemic pituitary gland, and sagging of the brain which can be remembered with the mnemonic SEEPS.³ These findings along with the appropriate clinical context can be used to

clinically diagnose a CSF leak and proceed with conservative treatment or epidural blood patching.³ In the event that first line treatment with conservative management or epidural patching is not helpful, further diagnostic imaging to localize a CSF leak can be performed.

There are 4 types of CSF leaks (**Table 2**), CSF leaks that are a result of dural tears are classified as type 1 (**Figs. 1 and 2**), a CSF leak resulting from a meningeal diverticulum is a type 2 CSF leak (**Fig. 3**), a type 3 CSF leak is due to a CSF-venous fistula (**Figs. 4 and 5**), and indeterminate CSF leaks are classified as type 4.¹ Brain and spine imaging play a critical role in the diagnosis of SIH. Historically, computed tomography (CT) myelogram has been the gold standard for detecting and localizing spinal CSF leaks.⁴ At our institution our approach is

^a Department of Imaging, Cedars-Sinai Medical Center; ^b Department of Imaging, Cedars Sinai Medical Center, 8700 Beverly Boulevard Taper Mezzanine M-335, Los Angeles, CA 90048; ^c Department of Neurosurgery, Cedars-Sinai Medical Center

* Corresponding author. Cedars Sinai Medical Center, 8700 Beverly Boulevard Taper Mezzanine M-335, Los Angeles, CA 90048.

E-mail address: Marcel.Maya@cshs.org

Table 1
Modified ICHD-3 diagnostic criteria for headache caused by spontaneous intracranial hypotension

Criterion	Description
A	Any headache attributed to low CSF pressure or CSF leakage that meets criterion C, below
B	Either or both of the following: <ul style="list-style-type: none"> • Low CSF pressure (<60 mm CSF) • Evidence of CSF leakage on imaging
C	Headache that developed in temporal relation to the low CSF pressure or CSF leakage or that led to its discovery
D	Headache not better accounted for by another ICHD-III diagnosis.

Abbreviation: CSF, cerebrospinal fluid; ICHD, International Classification of Headache Disorders

to first obtain MR brain with contrast and MR spine using heavily weighted T2 sequences (MR myelogram) as these studies have been shown to have similar sensitivity for identifying the presence of CSF leak.³⁻⁵ A flow diagram demonstrating our approach is shown in Fig. 6. MR brain and spine are favored for diagnostic purposes because of its noninvasive nature and the absence of radiation exposure. It is important to remember that up to 20% of patients with SIH have a normal brain MRI.³ In cases where patients who exhibit severe and disabling symptoms digital subtraction myelography (DSM) can be performed as it offers the highest sensitivity for identifying the leak site.⁶

In this article, we will discuss our experience and technique using DSM for the detection of CSF leaks with a focus on a 5-step mnemonic called the “5 P’s to success,” and potential diagnostic pitfalls to avoid.

Table 2
Classification of spontaneous spinal CSF leaks

Type 1	Dural tear <ul style="list-style-type: none"> a. Ventral b. (Postero-)lateral
Type 2	Meningeal Diverticulum <ul style="list-style-type: none"> a. Simple b. Complex/dural ectasia
Type 3	CSF-venous fistula
Type 4	Indeterminate

Abbreviation: CSF, cerebrospinal fluid

NORMAL ANATOMY AND IMAGING TECHNIQUE

CSF is a vital component of the central nervous system, distributed within the cerebral ventricles, and subarachnoid spaces of the brain and spinal cord. CSF production begins in the arachnoid plexus and is secreted into the cerebral ventricles. From there, CSF courses craniocaudally through the ventricular system in a unidirectional manner where it reaches the subarachnoid spaces, which is multidirectional, via the medial foramen of Magendie and the lateral foramina of Luschka. The mean volume of CSF is approximately 150 cc and regulated through production and absorption. Insufficient CSF volume can lead to intracranial hypotension, whereas excessive CSF volume can cause hydrocephalus. CSF is absorbed within the subarachnoid villi within the dural sinuses where it enters the systemic circulation. One of the primary functions of CSF is to “provide a hydromechanical protective role for the brain and spinal cord.”^{3,7}

The most common first line study ordered in the emergency setting for headaches is a noncontrast head CT.³ Although cranial CT has limited sensitivity, it is widely accessible and can potentially show signs of SIH such as basal cistern effacement, downward displacement of the cerebellar tonsils or subdural fluid collections. Effacement of the basal cisterns causes increased attenuation which is occasionally seen and can potentially be mistaken for a subarachnoid hemorrhage.

Initial imaging evaluation involves brain MRI and spinal MRI for the initial detection of CSF leaks.⁶ Traditionally, CT myelogram has been the gold standard for detecting CSF leaks; however, this has been supplanted by newer techniques such as dynamic CT myelogram and DSM for the accurate localization of CSF leaks.^{6,8} CT myelography involves the administration of intrathecal iodinated contrast after a lumbar puncture, followed by obtaining thin-cut CT images of the spine. However, 1 limitation of CT myelography is that in cases of high-flow CSF leaks, the extravasation of CSF can occur rapidly, leading to widespread distribution of the extradural CSF collection at the time of image acquisition that makes identifying a specific leak site challenging.^{9,10}

Brain MRI with intravenous contrast is an excellent initial test for the evaluation of SIH. It offers several advantages, including wide availability, absence of radiation exposure, and high sensitivity for detecting signs indicative of SIH. Specifically, it detects diffuse pachymeningeal enhancement in 73% of SIH patients.⁶ Brain MRI however does have its limitations, and it is important to remember that it can be normal in up to 20% of patients with SIH.^{3,6}

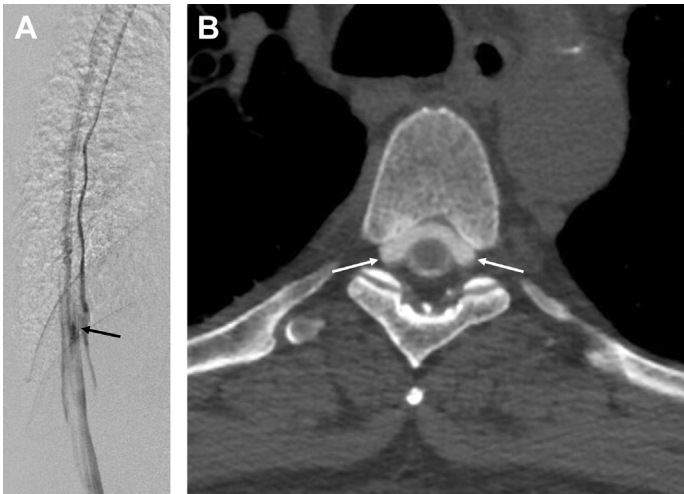


Fig. 1. 48-year-old male with bibrachial amyotrophy due to cerebrospinal fluid (CSF) leak. Prone digital subtraction myelography shows a ventral leak at the level of T9-10 (A, lateral projection). CT post myelogram of the thoracic spine shows large ventral extradural collection throughout the thoracic spine (B). Lateral projection DSM cine of ventral leak in another patient is provided in [Video 1](#).



Fig. 2. 23-year-old patient with a history of orthostatic headaches secondary to spontaneous intracranial hypotension (SIH). Digital subtraction myelography (DSM) in the left lateral decubitus positions shows a lateral leak at T4-5 (A). Corresponding MR myelography shows an extradural cerebrospinal fluid (CSF) collection at T4-5 (B). MRI of the thoracic spine shows circumferential CSF leak at this site (C). Frontal projection DSM cine is provided in [Video 2](#).

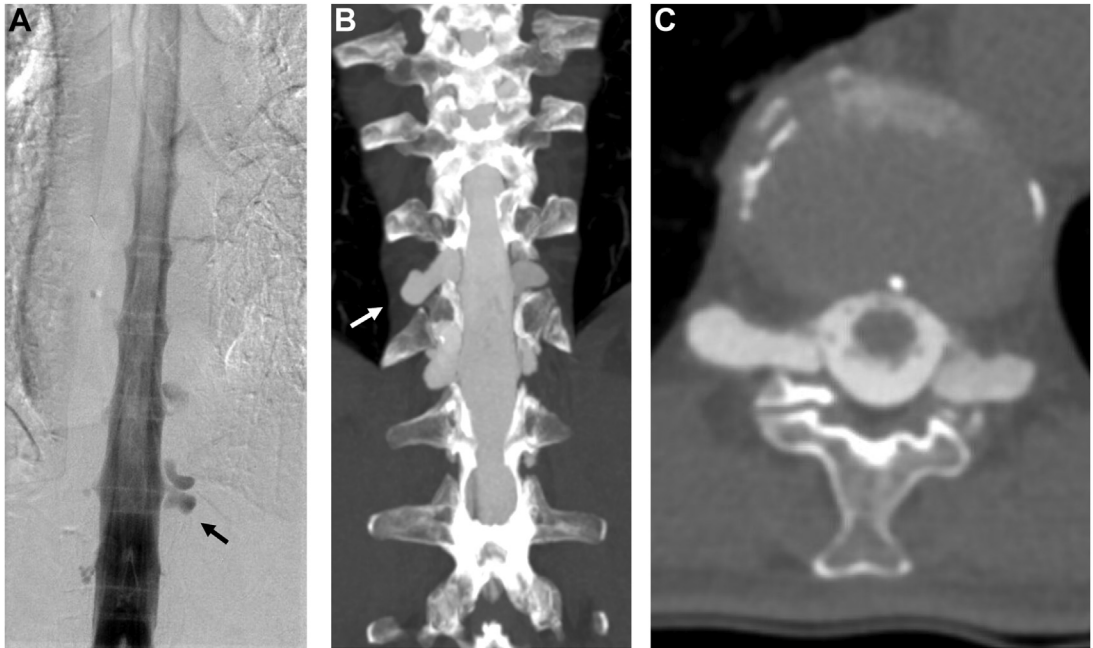


Fig. 3. 64-year-old patient with a history of SIH. Prone digital subtraction myelography (DSM) shows a meningeal diverticulum at T12-L1 (A, arrow). Post DSM CT myelography shows large thoracic nerve root cysts (B – coronal MIP, C – axial).

Spinal MRI can be performed using intrathecal gadolinium or with heavily weighted T2 sequences (Table 3). Heavily weighted T2 spinal MRI has demonstrated similar sensitivity to CT myelography, as reported in previous studies.¹¹ Intrathecal gadolinium spinal MR has not been shown to be superior to heavily weighted T2 spinal MR. Therefore, it is preferable to utilize spinal MRI with heavily weighted T2 sequences in conjunction with brain MR as part of the initial workup of SIH.^{6,12}

Digital subtraction myelogram is more invasive but has the highest sensitivity for localizing CSF leaks with comparable radiation dosing to CT myelogram.^{6,10} At our institution we now use DSM to identify and locate CSF leaks in a wider range of cases, including those with low-flow leaks which are typically reserved for CT myelogram. Based on our experience, DSM has demonstrated superior sensitivity compared to other imaging test in detecting CSF-venous fistulas and ventral leaks. Additionally, DSM has proven to be highly effective in precisely localizing the site of dural defect, providing valuable information for subsequent targeted treatment.^{3,13–15}

HISTORY

It is important to remember that spinal neuroimaging, although used for the initial diagnosis of CSF leak, has been found to yield negative results “in

48% to 76% of patients.”⁶ One potential explanation for the negative findings on spinal CT or MR imaging, particularly in cases where there are larger dural tears leading to extensive extrathecal contrast spanning multiple levels, is the limitation of temporal resolution. This limitation can make precise localization challenging. In 2003, Luetmer and Mokri introduced dynamic CT myelography to overcome this challenge.⁹ Although dynamic CT myelography offered improved temporal resolution, it still had limitations attributed “to the volume of tissue that must be imaged” as this leads to a higher radiation dose to the patient.^{8,16} In 2002, Philips, and colleagues,¹⁷ presented a case in which, despite utilizing conventional imaging techniques such as myelogram, CT myelogram or MRI, the authors were unable to identify a CSF leak. Since no leak was seen on imaging, a neurosurgical procedure was conducted, but it also failed to identify a leak. It was only when the authors performed a DSM, a novel technique at the time, that they were able to successfully diagnose a postoperative pseudomeningocele. Seven years after DSM was used to localize a pseudomeningocele, Hoxworth and colleagues used DSM to accurately identify high-flow CSF leaks.¹⁶ In the authors’ experience, conventional imaging techniques could detect the presence of a CSF leak, but due to the high-flow of the leaks, they were unable to precisely determine the location of CSF leak

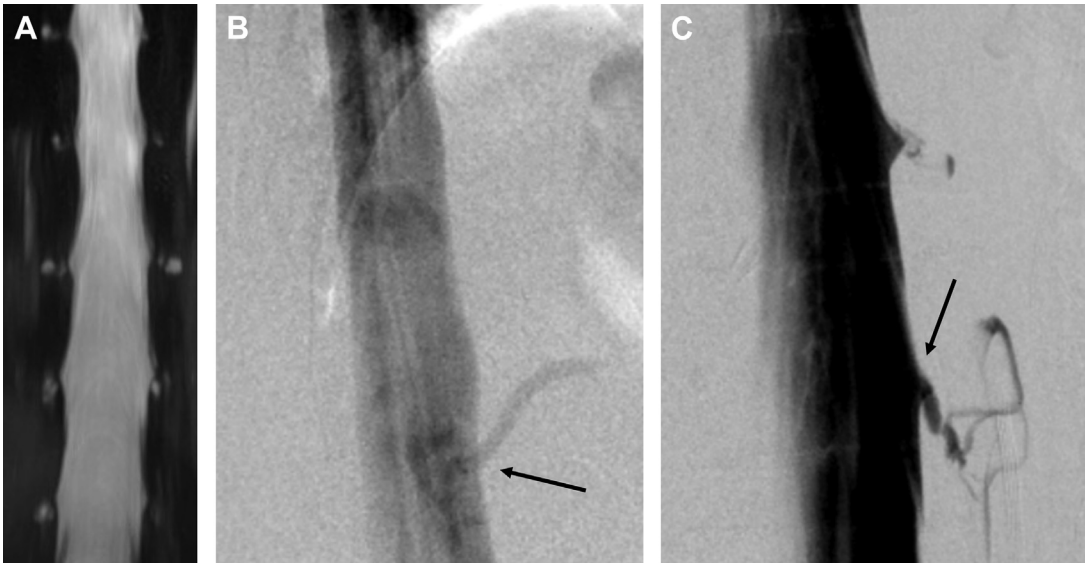


Fig. 4. 46-year-old patient with orthostatic headaches. MRI of the spine shows only small cyst without a cerebrospinal fluid (CSF) leak (A, MR myelography). The patient then underwent a left lateral decubitus digital subtraction myelogram which shows a CSF-venous fistula at T11 -12 (B, lateral projection, C, frontal projection).

without the higher temporal resolution provided by DSM. In 2012, Luetmer and colleagues⁸ proposed a new algorithm to determine which patients should undergo dynamic CT myelography. In their paper, the authors recommend that patients proceed directly to dynamic CT myelography if the initial spinal MR demonstrates an extradural CSF collection.⁸ At our institution, we adopted a comparable algorithm based on the presence or absence of spinal longitudinal extradural collections to determine the patient's positioning at DSM (Fig. 6).

In 2013, Schievink, and colleagues, showcased the utilization of DSM for the identification of a CSF-venous fistula in patients with SIH.¹⁴ At the time of the publication, this radiographic finding had not been previously reported. Beyond increased temporal resolution, DSM provides a diagnostic tool that offers about the same radiation dose as conventional CT myelography and about a third of the dose of dynamic CT myelography.¹⁸ In 2018 Farb and colleagues introduced the lateral decubitus position for DSM to increase the sensitivity of visualization of CSF venous fistulas.¹⁹ In their article, they categorized patients into the prone position if spinal MR showed an extradural CSF collection and the left lateral decubitus position if no extradural CSF collection was seen on spinal imaging. If the initial left lateral decubitus DSM was negative, the patient would return in a couple of weeks for a DSM on the contralateral side. This distinction between the presence of extradural CSF collection or not highlights the importance of pre-DSM planning.

APPROACH ("5 P'S TO SUCCESS")

Planning

At our institution, we have performed 2588 DSMs since 2009. Pre-DSM planning is imperative in the diagnosis and management of CSF leaks. The diagnostic process begins with MR brain to look for signs of intracranial hypotension and MR spine to determine for the presence of extradural fluid collections, as this will guide the patient's positioning during the subsequent DSM. Heavily T2 weighted myelographic sequences are important to determine positioning as the presence of large and/or irregular cysts will guide management to that specific spinal segment.²⁰ Based on the type of leak identified, the patient can be placed in various positions: prone for ventral leaks, lateral decubitus for lateral leaks, supine for posterior leaks, or lateral decubitus for CSF-venous fistulas.

Patient Preparation

Although DSM can be conducted with or without moderate sedation or general anesthesia, we prefer general endotracheal anesthesia with the patient in deep paralysis.²¹ In our experience this approach is well tolerated by patients while minimizing nondiagnostic examinations due to patient motion, but also ensures optimal detail and temporal resolution by facilitating controlled suspended respiration throughout the procedure. Three to 5 minutes prior to contrast bolus we ask the anesthesiologist to administer additional rocuronium to ensure full paralysis and avoid breathing attempts and

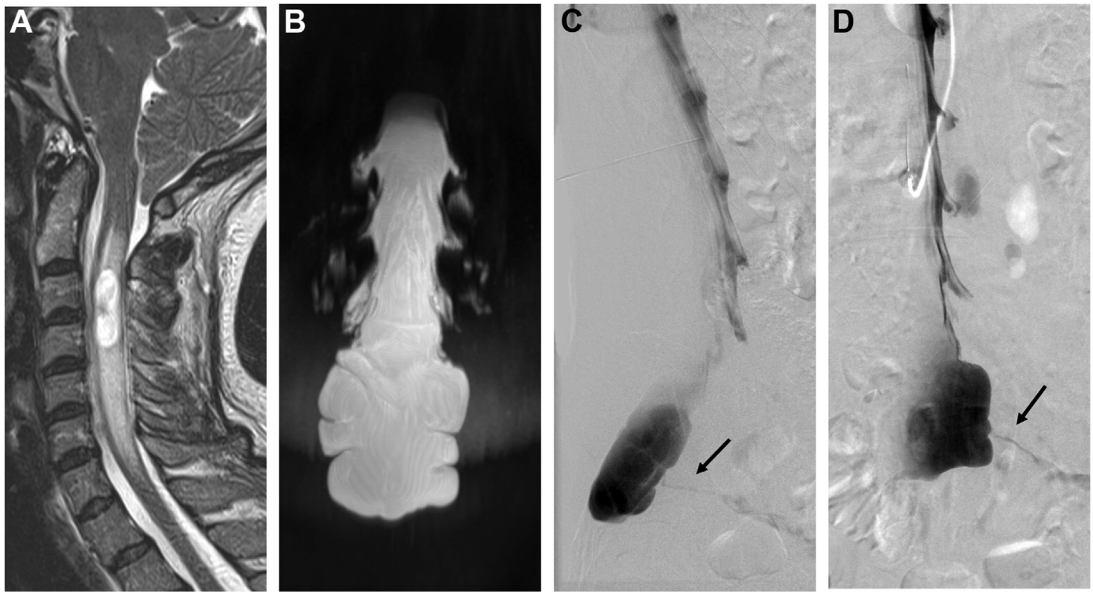


Fig. 5. 39-year-old patient with spontaneous intracranial hypotension (SIH) presented with upper extremity myelopathy and was found to have a spinal cord syrinx at C3-5 on MR C-spine (A). Initial workup revealed a large sacral Tarlov cyst on MR myelography (B) which was the focus of interrogation on subsequent digital subtraction myelography. Lateral projection (C) and ventral projection (D) Digital subtraction myelography (DSM) in the left lateral decubitus position show a cerebrospinal fluid (CSF)-venous fistula arising from the very large sacral Tarlov cyst at approximately the S2-3 level. Frontal and lateral projection DSM cine is provided in [Videos 3 and 4](#).

diaphragm spasms that may contribute to respiratory motion during image acquisition.

Positioning

Using a biplane angiography suite equipped with a tilt table, the patient can then be positioned in either the prone or lateral decubitus position. The table can then be adjusted to overcome lumbar lordosis and thoracic kyphosis. If the patient is in the prone position, this is done by tilting the table to greater than 15°. The lateral decubitus position requires less tilt than the prone position ([Fig. 7](#)). In the absence of tilt table, the patient can be

further positioned using pillows and custom wedges to help overcome lumbar lordosis.²¹ To enhance the diagnostic yield of DSM for the diagnosis CSF-venous fistulas, patients are positioned in the lateral decubitus position. In our institutional experience, we have demonstrated that this position increased our diagnostic yield from 15% to 75%.¹⁵

Puncture

Under fluoroscopic guidance, a Gertie-Marx 22-gauge needle is placed midline at the L2-3 level taking caution to avoid tenting and prevent a subdural injection. Opening pressure is then obtained and 0.5 cc of iohexol 240 mg/mL or 300 mg/mL contrast (Omnipaque; GE Healthcare, Marlborough, Massachusetts) is injected to determine needle position. Once the intradural position of the needle is confirmed during the procedure, the patient can then be repositioned to optimize the diagnostic yield and concentrate on a specific region of greatest interest. This repositioning allows for a more targeted approach, enhancing the accuracy and effectiveness of the procedure.

Procedure Imaging

Images are acquired at a frame rate of 1 frame per second using a 75 second breath hold with manual

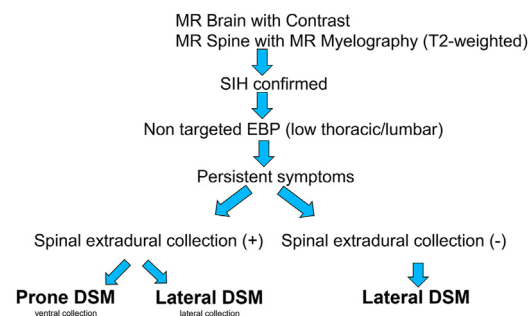


Fig. 6. Cedars-Sinai diagnostic approach for patients with suspected spontaneous intracranial hypotension (SIH).

Table 3
Imaging protocols

CT brain without contrast	Helical scan at 0.5 s tube rotation with 0.625 thickness 2 mm reformats in the sagittal and coronal plane
CT myelogram	Helical scan at 1 s tube rotation with 0.625 thickness for cervical spine Helical scan at 0.6 s tube rotation with 0.625 thickness for thoracic and lumbar spine 2 mm reformats in the sagittal and coronal plane
Dynamic CT myelogram	Dynamic CT myelogram can be performed in various positions and with rapid repositioning to elucidate otherwise difficult to detect leaks Helical scans at 0.6 s tube rotation with 2.5 mm thickness Five scan acquisitions in the prone (arms up), left lateral decubitus, right lateral decubitus, prone (arms up), supine (arms up)
MR brain with and without contrast	Sagittal T1, axial diffusion weighted imaging, axial FLAIR, axial T2, coronal T2 FS, axial susceptibility-weighted imaging, sagittal T2, axial T1 MPRAGE post, sagittal MPR post, Coronal MPR post
MR spine with myelogram	Sagittal T1, sagittal T2, sagittal STIR, axial T2, and coronal T2 haste with 3D, sagittal T1 post FS, and 3D maximum intensity projection reconstructions
Digital subtraction myelogram	Digital subtraction fluoroscopy during intrathecal contrast injection Performed with general endotracheal anesthesia

injection of 12 cc of iohexol 240 mg/mL or 300 mg/mL at a rate of 1 cc per second. This is followed by a 20 cc saline flush. It is our standard practice that all patients undergo a CT myelogram 1-hour post-DSM. This additional imaging procedure is essential and complements the diagnostic process. A recent article by Lutzen, and colleagues, demonstrated a novel use of ultrahigh-resolution cone-beam CT (UHR-CBT) following DSM to identify a CSF venous fistula in a patient with negative MR spine and CT myelogram.²² While it is unclear if the CSF venous

fistula was diagnosed during the preceding DSM, the increased spatial resolution achieved with UHR-CBT provides an additional tool to add to the growing arsenal of techniques being developed and advancing the field of spinal CSF leak localization.

PITFALLS AND LIMITATIONS

False Localizing Signs

During the pre-DSM planning phase, fluid collections in the upper cervical spine at the C1-2 level are occasionally observed on spinal imaging (Fig. 8). It has been commonly believed that these fluid collections correspond to the site of CSF leak and treatment has been directed at the C1-2 level.^{23–25} Yousry and colleagues²⁶ were the first to propose that these retrospinal fluid collections did not accurately represent the site of CSF leak but rather represented fluid collections caused by paraspinal venous transudate or exudate. Schievink and colleagues²⁷ found that these retrospinal fluid collections did indeed originate from CSF leakage from the epidural space that then extend cranially where they ultimately extravasate into the surrounding C1-2 soft tissues.²⁸ It is important to recognize this distinction to avoid inadvertently directing therapy at the wrong level. A paraspinal fluid collection at the high cervical region has been termed the “false localizing sign of C1-2.”²⁷

Another false localizing sign that has been previously described is contrast extravasation in the



Fig. 7. Biplane angiography suite equipped with a tilt table. The angle of the table is greater than 15°.

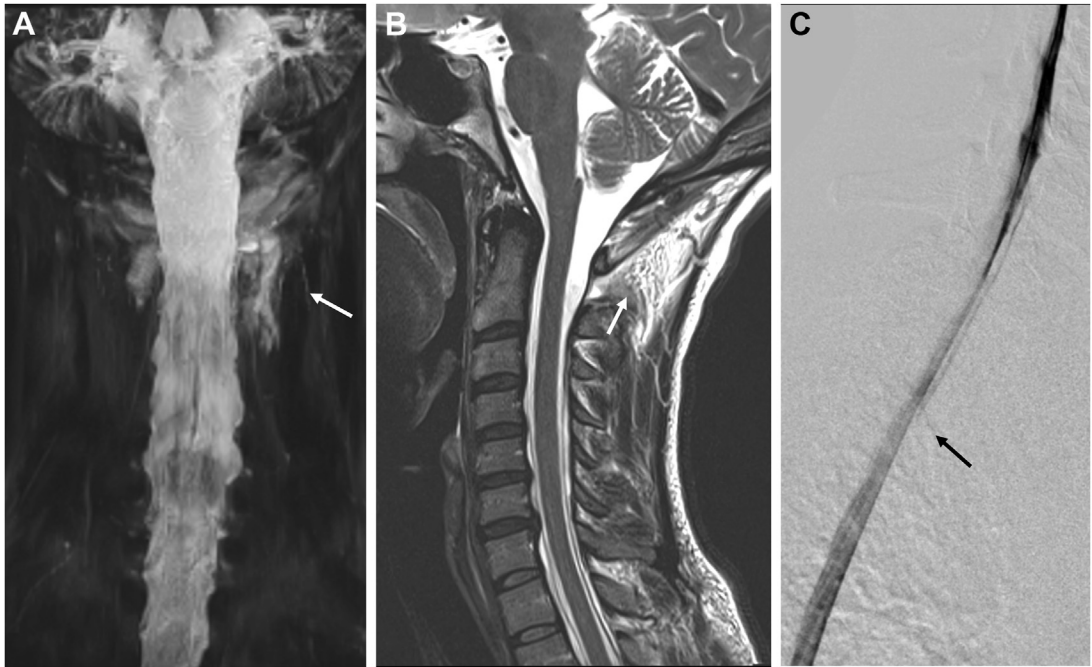


Fig. 8. 40-year-old patient with spontaneous intracranial hypotension (SIH). MR myelography (A) and sagittal T2 MR of the cervical spine (B) show extensive extradural cerebrospinal fluid (CSF) collection in the posterior soft tissues of the upper cervical spine consistent with false localizing sign of C1-2. Subsequent digital subtraction myelography (DSM) in the prone position (lateral projection) shows the site of ventral CSF leak to be at T2-3 (C).

cervicothoracic region. A study at our institution looking at 11 patients with preplanning imaging showing fluid collections at the cervicothoracic region demonstrated that these fluid collections were not indicative of the site of leak.²⁹ As a result, treatment targeted at the region of fluid collection in the cervicothoracic region is not likely to result in prolonged symptom improvements for patients. This finding has been termed the false localizing sign of cervicothoracic CSF leak (Fig. 9).

Although MR myelography is the preferred initial imaging of choice, up to 50% of SIH cases have negative spinal imaging.⁶ Patients with CSF-venous fistulas are more likely to have no CSF leak identified on conventional imaging. Not all patients undergo DSM, therefore, it is important to recognize secondary findings that suggest the presence of CSF-venous fistula on CT myelography. One of those signs is the presence of a hyperattenuating paraspinal vein which has been appropriately named the “hyperdense paraspinal vein sign.”³⁰ While initially thought to correspond to the level of CSF-venous fistula localization, Schievink, and colleagues,³¹ demonstrated a case of 2 patients with hyperdense paraspinal veins who underwent treatment with surgery or glue injection whose CSF-venous fistula was not at the same level or laterality as the draining veins. The authors

concluded that while the hyperdense paraspinal vein sign was indicative of a CSF-venous fistula, consideration should be given to DSM or dynamic myelography prior to treatment to avoid the potential pitfall of directing treatment at the incorrect site. This potential pitfall is known as the false localizing sign of CSF-venous fistulas.³¹

Skull Base Leaks Do Not Cause Spontaneous Intracranial Hypotension

In 2012, Schievink, and colleagues,³² conducted a study with the aim of investigating the potential causal association between cranial CSF leaks and SIH. The authors identified 315 patients over a 9-year period and found no evidence to suggest that SIH was caused by base of skull CSF leaks. Instead, they concluded that “clear nasal discharge in patients with SIH can be considered a false localizing sign.”³² It took almost 10 years for Schievink and colleagues to utilize lateral decubitus DSM and discover a rapid-flow CSF leak at the posterior fossa that drained into the subclavian vein in a 2-year old boy.³³ Historically, skull-based CSF leaks were thought not to be a cause of SIH. While unusual to have a CSF leak not located within the spine, this case suggests that CSF leaks from the posterior fossa can cause SIH, albeit



Fig. 9. 43-year-old patient with orthostatic headaches. MR T-spine (A) shows dorsal (arrow) and ventral (arrowhead) epidural fluid collections. Heavily T2-weighted spinal MRI MIP images (B) show a complex meningeal diverticulum at T10 to 11 (arrow) and false localizing sign of the cervicothoracic spine (arrowhead). Digital subtraction myelography in the left lateral decubitus position (frontal projection) show epidural cerebrospinal fluid (CSF) leak associated with a lateral tear at T9-10 meningeal diverticulum.

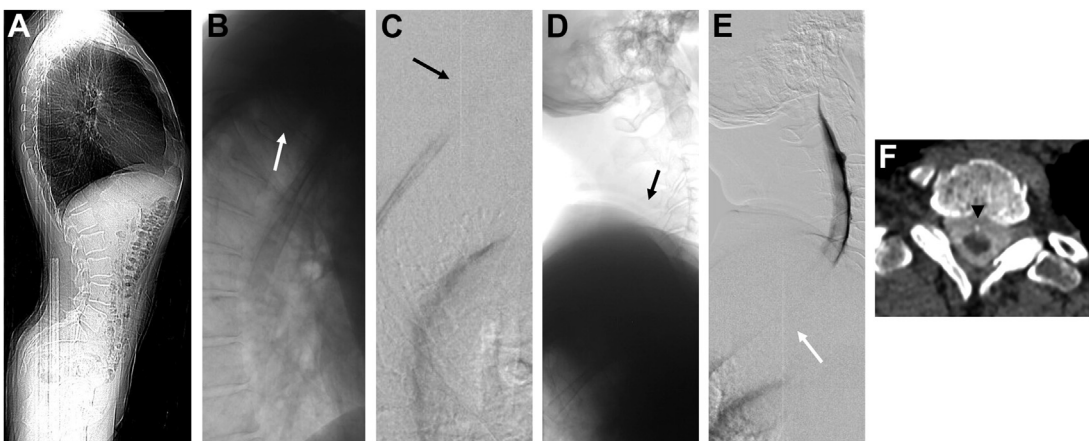


Fig. 10. Scout image demonstrates thoracic kyphosis and lumbar lordosis (A). Digital subtraction myelography (DSM) without bone suppression (B, D) and with bone suppression (C, E) show under penetration of the spine at the cervicothoracic region with poor visualization of the contrast column at this level. Post DSM CT myelogram shows calcification at the site of the dural tear (F).

rarely. Another potential pitfall related to CSF leaks is a subset of patients who in addition to having headaches and SIH, have clear nasal discharge.³² It is important for clinicians to have a high index of suspicion for SIH in patients with skull-based CSF leaks, as delayed diagnosis and treatment can have debilitating consequences.^{33,34}

Venolymphatic Vascular Malformations

Thus far we have discussed CSF-venous fistulas in the context of high-flow leaks, but they can also be associated with slow-flow vascular anomalies. For example, in 2014, Mokri reported 2 cases of patients with CSF leaks and Klippel-Trenaunay-Weber syndrome.³⁵ Since then, 5 cases of patients with venous/venolymphatic vascular malformations and SIH have been identified; 3 patients had venous/venolymphatic malformations, 1 patient had a venous malformation (hemangioma), and the last patient had a pelvic/sacral vascular malformation.^{36–38} Although there is no definitive causal relationship between venolymphatic vascular malformations and SIH, it is important to include the diagnosis in the differential when both conditions are observed simultaneously.

Limitations

One of the limitations inherent to DSMs is the limited field of view which may not cover the entire spinal column. In this instance, a repeat procedure may be necessary. Additional DSM is also required to assess CSF venous fistulas in lateral decubitus positions on different days.²¹ While most CSF venous fistulas are apparent within 60 seconds of DSM run,²⁰ some ventral leaks are too slow to visualize during the 60 to 80 seconds DSM run. For these slower leaks, dynamic CT myelogram with imaging at longer intervals may be more appropriate.^{9,10} Additionally, given different body habitus, there are certain anatomic areas which are inherently more difficult to evaluate such as the cervicothoracic region overlying the shoulders (**Fig. 10**). Future refinements in technique may overcome some of the limitations which include newer equipment with increased detector size and cone beam CT which has been used to detect slow flow leaks not detected on DSM.³⁹

SUMMARY

SIH is an important cause of orthostatic headache. The most prevalent identifiable cause of SIH is a CSF leak occurring in the spinal column. Digital subtraction myelography is the most sensitive imaging technique for pinpointing the precise location of the CSF leak. Moreover, DSM is well tolerated

with radiation doses comparable to those of CT myelography.

CLINICS CARE POINTS

- Digital subtraction myelography has high sensitivity for identifying leak site.
- A hyperdense paraspinous vein sign on CT myelography may be a false localizing sign of CSF-venous fistulas.
- Paraspinous fluid in the C1-2 region does not correspond to site of CSF leak and is known as the false localizing sign of C1-2.
- CSF leaks in the cervicothoracic region seen on spinal imaging are rarely the site of leak and targeted treatment in this region is not likely to result in lasting symptom relief.
- While rare, skull-based CSF leaks can cause SIH.

DISCLOSURE

The authors have nothing to disclose.

SUPPLEMENTARY DATA

Supplementary data related to this article can be found online at <https://doi.org/10.1016/j.rcl.2023.10.004>

REFERENCES

1. Schievink WI, Maya MM, Jean-Pierre S, et al. A classification system of spontaneous spinal CSF leaks. *Neurology* 2016;87(7):673–9.
2. Schievink WI, Maya MM, Moser FG, et al. Incidence of spontaneous intracranial hypotension in a community: Beverly hills, California, 2006–2020. *Cephalalgia* 2022;42(4–5):312–6.
3. Chan SM, Chodakiewitz YG, et al. Intracranial hypotension and cerebrospinal fluid leak. *Neuroimaging Clin* 2019;29(2):213–26.
4. Schievink WI. Novel neuroimaging modalities in the evaluation of spontaneous cerebrospinal fluid leaks. *Curr Neurol Neurosci Rep* 2013;13(7):358.
5. Tay ASS, Maya M, Moser FG, et al. Computed tomography vs heavily T2-weighted magnetic resonance myelography for the initial evaluation of patients with spontaneous intracranial hypotension. *JAMA Neurol* 2021;78(10):1275–6.
6. D'Antona L, Merchan MAJ, Vassiliou A, et al. Clinical presentation, investigation findings, and treatment outcomes of spontaneous intracranial hypotension

- syndrome. *JAMA Neurol* 2021;78(3). <https://doi.org/10.1001/jamaneurol.2020.4799>.
7. Sakka L, Coll G, Chazal J. Anatomy and physiology of cerebrospinal fluid. *European Annals of Otorhinolaryngology, Head and Neck Diseases* 2011;128(6):309–16.
 8. Luetmer PH, Schwartz KM, Eckel LJ, et al. When should I do dynamic CT myelography? predicting fast spinal CSF leaks in patients with spontaneous intracranial hypotension. *Am J Neuroradiol* 2012;33(4):690–4.
 9. Luetmer PH, Mokri B. Dynamic CT myelography: A technique for localizing high-flow spinal cerebrospinal fluid leaks. *Am J Neuroradiol* 2003;24(8):1711–4.
 10. Kranz PG, Luetmer PH, Diehn FE, et al. Myelographic techniques for the detection of spinal CSF leaks in spontaneous intracranial hypotension. *Am J Roentgenol* 2016;206(1):8–19.
 11. Wang Y, Lirng J-, Fuh J-, et al. Heavily T2-weighted MR myelography vs CT myelography in spontaneous intracranial hypotension. *Neurology* 2009;73(22):1892–8.
 12. Dobrocky T, Winklehner A, Breiding PS, et al. Spine MRI in spontaneous intracranial hypotension for CSF leak detection: Nonsuperiority of intrathecal gadolinium to heavily T2-weighted fat-saturated sequences. *Am J Neuroradiol* 2020;41(7):1309–15.
 13. Schievink WI, Moser FG, Maya MM, et al. Digital subtraction myelography for the identification of spontaneous spinal CSF-venous fistulas. *J Neurosurg Spine* 2016;24(6):960–4.
 14. Schievink WI, Moser FG, Maya MM. CSF-venous fistula in spontaneous intracranial hypotension. *Neurology* 2014;83(5):472–3.
 15. Schievink WI, Maya MM, Moser FG, et al. Lateral decubitus digital subtraction myelography to identify spinal CSF-venous fistulas in spontaneous intracranial hypotension. *J Neurosurg Spine* 2019;31(6):1–905.
 16. Hoxworth JM, Patel AC, Bosch EP, et al. Localization of a rapid CSF leak with digital subtraction myelography. *Am J Neuroradiol* 2009;30(3):516–9.
 17. Phillips CD, Kaptain GJ, Razack N. Depiction of a postoperative pseudomeningocele with digital subtraction myelography. *Am J Neuroradiol* 2002;23(2):337–8.
 18. Nicholson PJ, Guest WC, van Prooijen M, et al. Digital subtraction myelography is associated with less radiation dose than CT-based techniques. *Clin Neuroradiol* 2021;31(3):627–31.
 19. Farb RI, Nicholson PJ, Peng PW, et al. Spontaneous intracranial hypotension: A systematic imaging approach for CSF leak localization and management based on MRI and digital subtraction myelography. *Am J Neuroradiol* 2019;40(4):745–53.
 20. Mark I, Madhavan A, Oien M, et al. Temporal characteristics of CSF-venous fistulas on digital subtraction myelography. *Am J Neuroradiol* 2023;44(4):492–5.
 21. Kim DK, Brinjikji W, Morris PP, et al. Lateral decubitus digital subtraction myelography: Tips, tricks, and pitfalls. *Am J Neuroradiol* 2020;41(1):21–8.
 22. Lützen N, Beck J, Urbach H. Cerebrospinal fluid venous fistula imaging with ultrahigh-resolution cone-beam computed tomography. *JAMA Neurol* 2023. <https://doi.org/10.1001/jamaneurol.2023.1640>.
 23. Beck J, Raabe A, Seifert V, et al. Intracranial hypotension after chiropractic manipulation of the cervical spine. *J Neurol Neurosurg Psychiatr* 2003;74(6):821–2.
 24. Kamada M, Fujita Y, Ishii R, et al. Spontaneous intracranial hypotension successfully treated by epidural patching with fibrin glue. *Headache* 2000;40(10):844–7.
 25. Kasner SE, Rosenfeld J, Farber RE. Spontaneous intracranial hypotension: Headache with a reversible Arnold-Chiari malformation. *Headache* 1995;35(9):557–9.
 26. Yousry I, Forderreuther S, Moriggl B, et al. Cervical MR imaging in postural headache: MR signs and pathophysiological implications. *Am J Neuroradiol* 2001;22(7):1239–50.
 27. Schievink WI, Maya MM, Tourje J. False localizing sign of C1–2 cerebrospinal fluid leak in spontaneous intracranial hypotension. *J Neurosurg* 2004;100(4):639–44.
 28. Schievink WI, Maya MM, Moser F, et al. Multiple spinal CSF leaks in spontaneous intracranial hypotension: Do they exist? *Neurology. Clin Pract* 2021;11(5):e691–7.
 29. Schievink WI, Maya MM, Chu RM, et al. False localizing sign of cervico-thoracic CSF leak in spontaneous intracranial hypotension. *Neurology* 2015;84(24):2445–8.
 30. Kranz PG, Amrhein TJ, Schievink WI, et al. The hyperdense paraspinous vein sign: A marker of CSF-venous fistula. *Am J Neuroradiol* 2016;37(7):1379–81.
 31. Schievink WI, Maya MM, Moser FG. False localizing signs of spinal CSF-venous fistulas in spontaneous intracranial hypotension: Report of 2 cases. *J Neurosurg Spine* 2019;31(5):1–767.
 32. Schievink WI, Schwartz MS, Maya M, et al. Lack of causal association between spontaneous intracranial hypotension and cranial cerebrospinal fluid leaks: Clinical article. *J Neurosurg* 2012;116(4):749–54.
 33. Schievink WI, Michael LM, Maya M, et al. Spontaneous intracranial hypotension due to Skull-Base cerebrospinal fluid leak. *Ann Neurol* 2021;90(3):514–6.
 34. Schievink WI. Spontaneous intracranial hypotension. *N Engl J Med* 2021;385(23):2173–8.
 35. Mokri B. Klippel-trenaunay-weber syndrome (KTWS) and spontaneous spinal CSF leak: Coincidence or link. *Headache* 2014;54(4):726–31.
 36. Schievink WI, Maya MM, Moser FG, et al. Spontaneous spinal CSF-venous fistulas associated with venous/

- venolymphatic vascular malformations: Report of 3 cases. *J Neurosurg Spine* 2019;32(2):305–10.
37. Chan JL, Maya MM, Schievink WI. Open repair of Hemangioma-Associated cerebrospinal Fluid-Venous fistula. *Ann Neurol* 2021;89(3):621–2.
 38. Schievink WI, Maya MM, Borst AJ. Adolescent headache due to congenital pelvic/sacral vascular malformation. *Ann Neurol* 2023. <https://doi.org/10.1002/ana.26651>.
 39. Lützen N, Demerath T, Volz F, et al. Conebeam CT as an additional tool in digital subtraction myelography for the detection of spinal lateral dural tears. *Am J Neuroradiol* 2023;44(6):745–7.